Supporting Information

Molecular metal oxide clusters soldered interpenetrating polymer network 'hosts' carbon nanotube 'guest' for green millimeter wave absorption

Kunal Manna,[#, †,] Ria Sen Gupta,[#] Samir Mandal, Arya Swaminadhan, Soumi Dutta, Ketaki Samanta, Sk Safikul Islam, Amit Malakar, and Suryasarathi Bose[†,*]*

[†]Department of Materials Engineering, Indian Institute of Science, Bengaluru – 560012, India

** Corresponding Author Email address (kunalchemi17@gmail.com, sbose@iisc.ac.in)*

Supporting Information I (SI-1)

Characterization Techniques:

The constructs were characterized via Fourier Transform IR spectroscopy (FTIR) from PerkinElmer Frontier in the range of mid-IR. X-ray photoelectron spectroscopy was performed on Axis Ultra with Al as the monochromatic source (1.486 keV). Morphological studies and elemental analysis were performed using Ultra55 FE-SEM Karl Zeiss scanning electron microscope equipped with an EDX detector and transmission electron microscope (TEM, FEI Technai G2). Thermogravimetric analysis was performed using TA Q500. XRD (X-ray Diffraction) analysis was performed using PANalytical X-Pert PRO instrument equipped with Cu K_α radiation (λ=1.54 A°). Raman analysis was duly performed using LabRAM HR with CCD detector. The Zeta-potentials of the particles and the membranes were evaluated using a Zeta-potential analyzer (Zetasizer NanoZS90, Malvern Instruments) and an electro-kinetic analyzer, SurPASS, Anton Par. BET surface area analysis was carried out in MicrotracBEL, Corp and the corresponding data were analyzed using BELSORP Data Analysis Software BELMaster - Ver 7.3.2.0. The electrical conductivities at room temperature of the constructs and control samples were measured on uniformly polished and compression-molded disks of a thickness of 1 mm via an Alpha-N analyzer, Novocontrol (Germany), with Vrms at 1 V in a wide frequency range of 0.1 Hz to 10 MHz. The EMI shielding properties of the constructs and the control samples were measured using an Agilent vector network analyzer (VNA) in X, K_u and K band (freq. range = 8.2 to 26.5 GHz). The VNA was coupled to a Vidyut Yantra Udyog (model KU7061; S.N. 2454) waveguide. The bending fatigue test was carried out using a home-built bending fatigue test unit with a bending radius and frequency of 10 mm and 1 Hz, respectively.

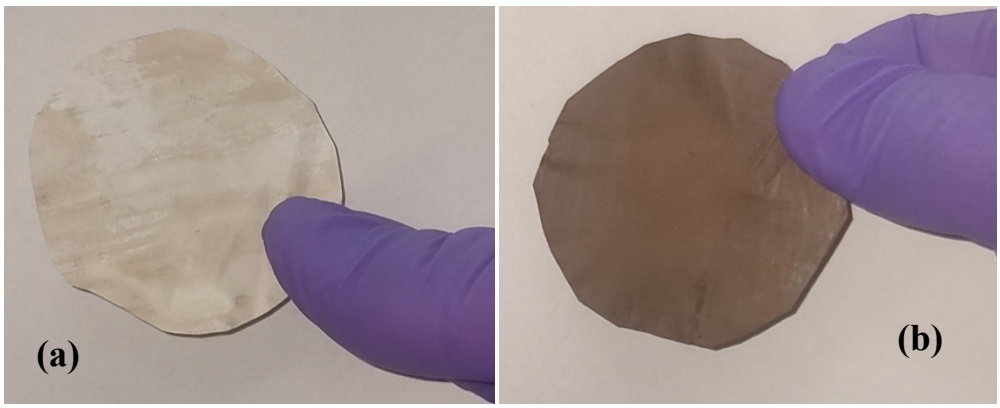

Figure S1. Digital image of freestanding (a) IPN membrane and (b) Cu-POM infused IPN membrane.

Figure S1a depicts the digital image of the PVDF/Polydopamine IPN membrane. The slight off-white appearance of the IPN membrane indicates the formation of the sequential interpenetrating polymeric network composed of polydopamine in the PVDF matrix in the coagulation bath containing a solution of Tris buffer (10 mM, pH = 8.5) and NaIO4 (5 mM) at 4 °C. However, in Figure S1b the brownish color of the membrane is due to the homogeneous distribution of negatively charged Keggin-type Cu-POMs which was electrostatically tagged to the counter-charged Dopamine.HCl (positively charged) monomers during membrane fabrication, and this dopamine upon polymerization helps in carrying the Cu-POMs throughout the network of IPN, not only on the membrane surface but also inside the pores.

Supporting Information II (SI-2)
DMA Analysis:

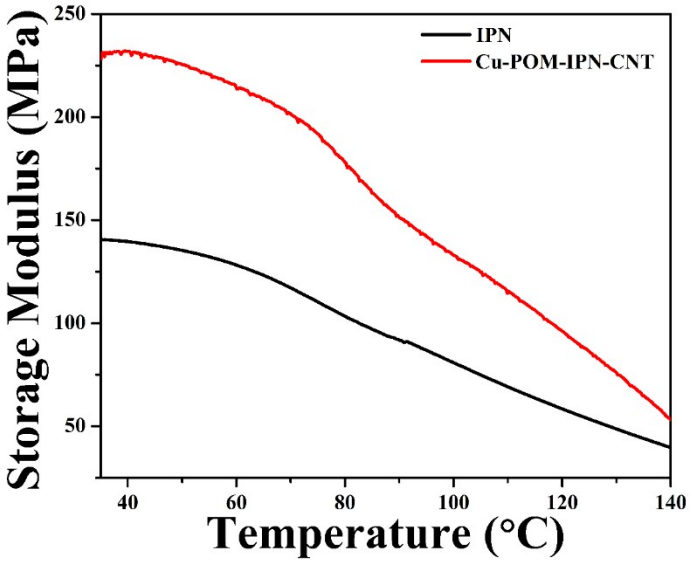

Figure S2: DMA curves depicting the mechanical integrity of neat IPN and Cu-POM-IPN-CNT construct

The mechanical stability of the prepared constructs was probed via dynamic mechanical analysis. From the DMA data, we see that the neat IPN membranes exhibited a storage modulus of nearly 140 MPa. Whereas upon infusion of the Cu-POM immobilized CNT hybrid into the sequential IPN matrix, a significant jump was observed in terms of storage modulus (c.a. 230 MPa). This essentially stems from the fact that the infused modified CNTs successfully reinforced the already stable IPNs and resulted in such elevated storage modulus values. This high storage modulus contributes to the overall robustness and usability of the material over a wide range of harsh operational conditions. Here in Figure S2, we can see that with increasing the temperature, storage modulus decreases. This behavior may be due to the softening effect of the polymer at high temperature. Therefore, secondary forces of the chain reduce with increasing temperature and enhances the chain mobility and reduces the storage modulus.

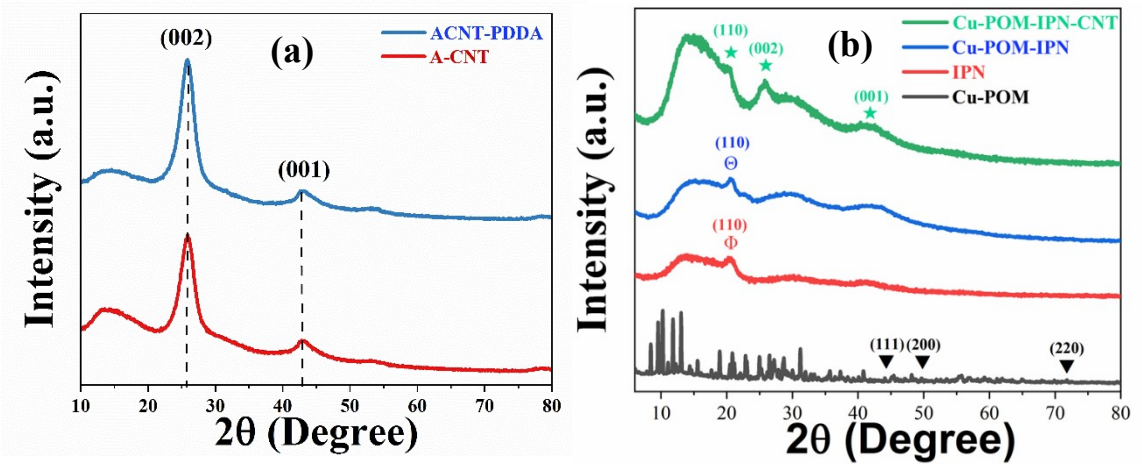

Figure S3: XRD plot of (a) ACNT and ACNT/PDDA, (b) Cu-POM, IPN, Cu-POM-IPN and Cu-POM-IPN-CNT.

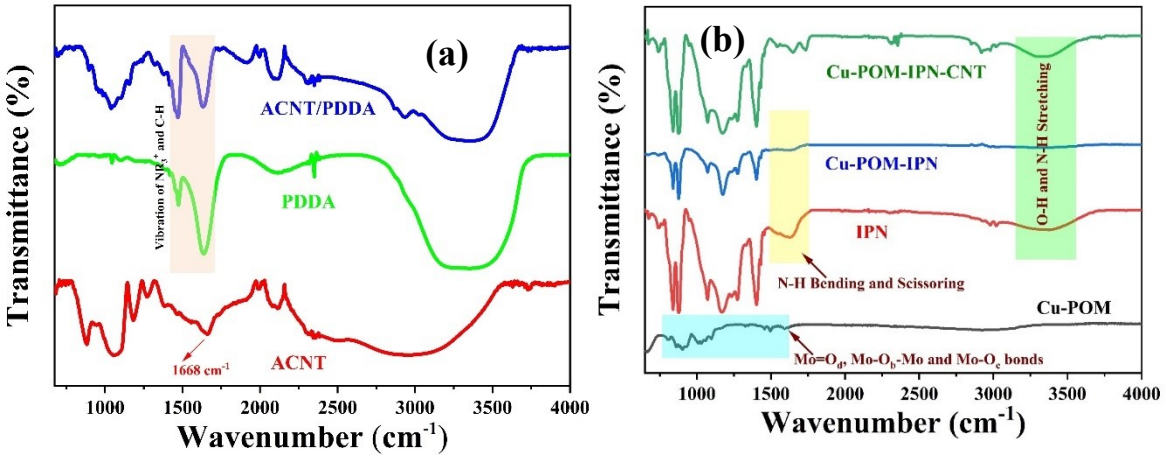

Figure S4: FTIR spectra of (a) ACNT, PDDA and ACNT/PDDA, (b) Cu-POM, IPN, Cu-POM-IPN and Cu-POM-IPN-CNT.

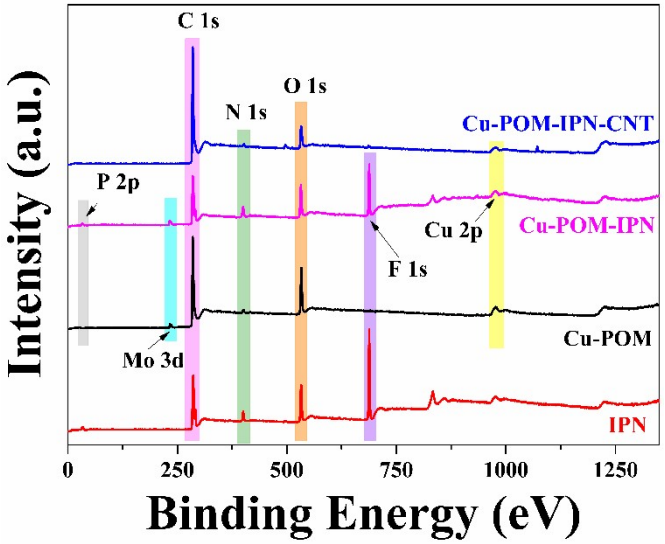

Figure S5: XPS survey scan spectra of IPN, Cu-POM, Cu-POM-IPN, Cu-POM-IPN-CNT.

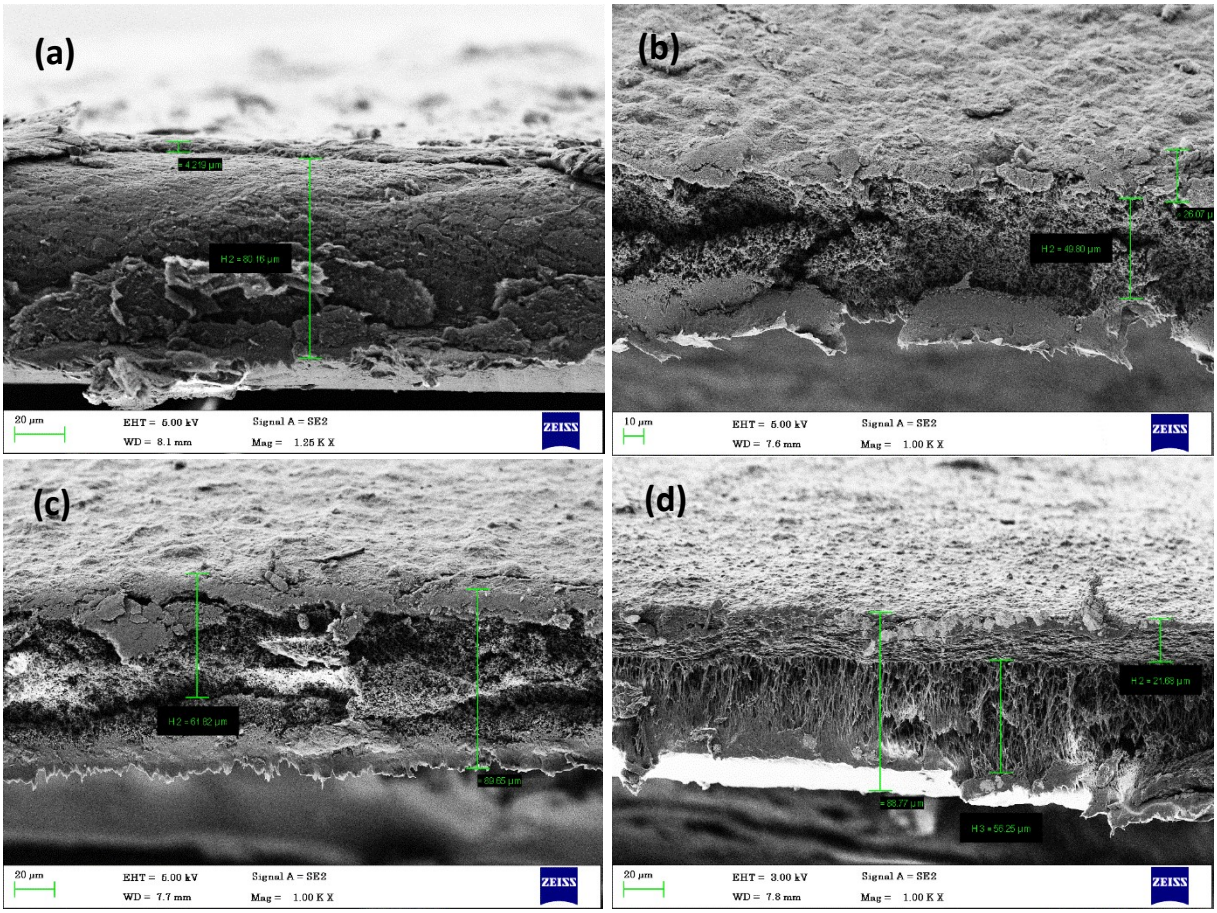

Figure S6. Cross-section SEM images for constructs with different deposition thickness (a) 5 mg (b) 10 mg, (c) 15 mg, and (d) 20 mg, respectively.

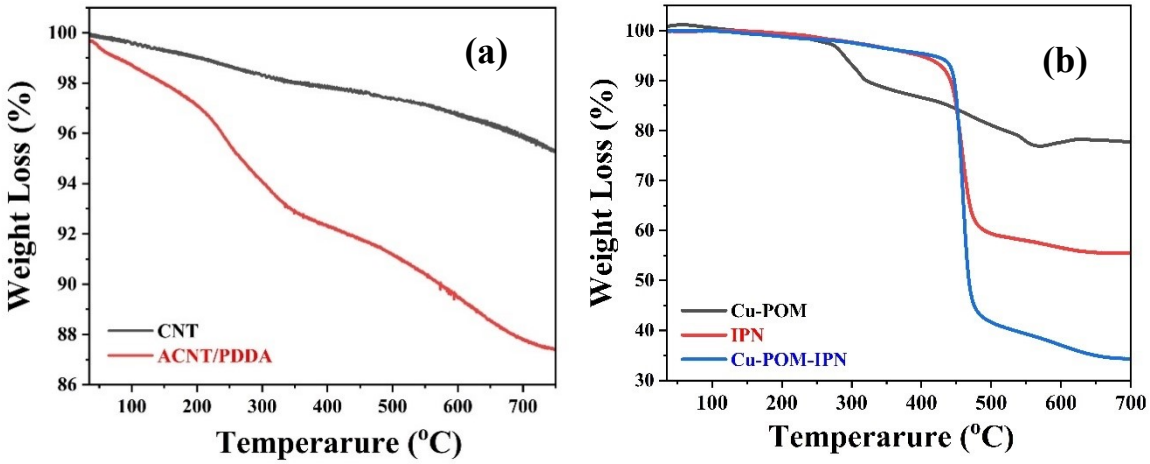

Figure S7. TGA curves of (a) pristine CNT and ACNT/PDDA powder. (b) Cu-POM, IPN, and Cu-POM-IPN-CNT construct.

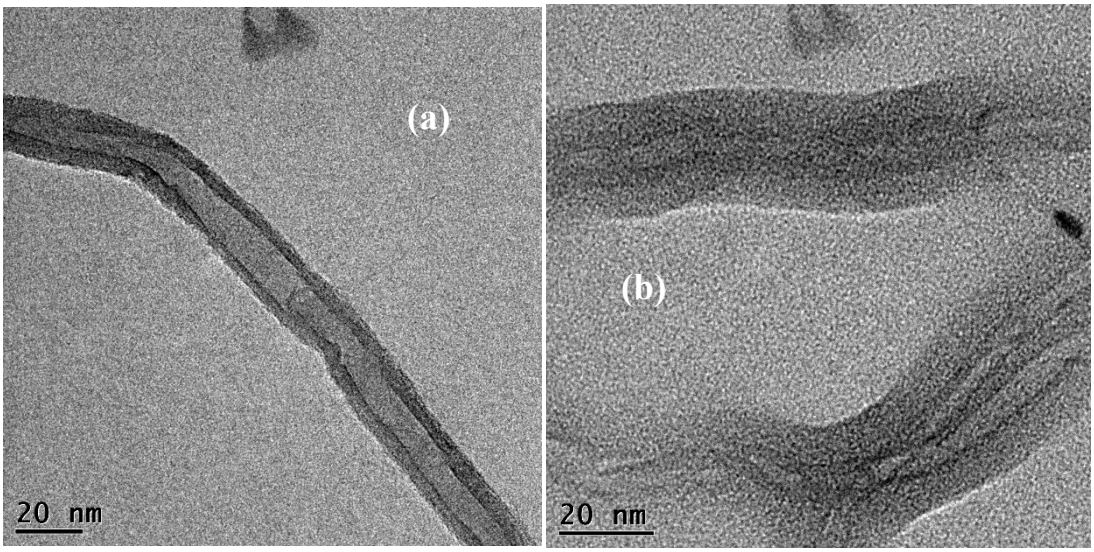

Figure S8: TEM images of (a) ACNT and (b) ACNT/PDDA.

Table S1: Coverage Density (chain/nm^2) of PDDA on ACNT

Sample	Linker	MW (g/mol)	W_{loss}%	SSA_{BET} (m^2g^{-1})	ρ (molecules/nm^2)
ACNT/PDDA	-COOH	491.06	12	189	1.058

Supplementary Information III (SI-3)

BET Plot

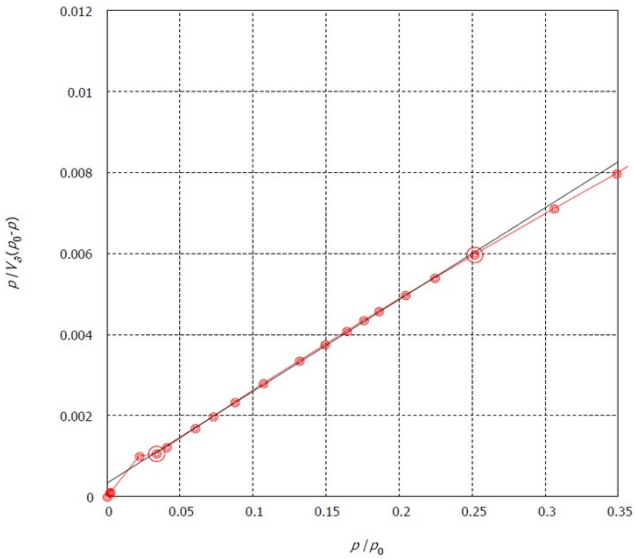

BET-Plot

Adsorptive N2

Adsorption temperature 77.000 [K]

V_m	43.477	[cm³(STP) g⁻¹]	$a_{S,BET}$	1.8923E+02	[m² g⁻¹]
C	67.217		Total pore volume (p/p_0=0.9032)	0.3781	[cm³ g⁻¹]
			Average pore diameter	7.9925	[nm]

Figure S9. BET Plot and data of ACNT/PDDA.

To check the dispersibility of CNTs, ACNTs and ACNT-PDDA in water and the stability of the aqueous suspension of 1 mg/ml concentration they are sonicated using a probe sonicator for 20 min and then kept for 1 month. Digital image of the aqueous dispersion of CNT, ACNT and ACNT/PDDA was captured immediately after the dispersion was prepared through probe sonication (a) and dispersion after 1 month (b). From Figure S10 a and b it is evident that acid treatment followed by PDDA coating effectively facilitates uniform dispersibility of ACNT and ACNT/PDDA in polar solvents through positive charge of cationic liquid PDDA. In addition to that induction of nanoscale defects and functional groups on the surface of pristine MWCNTs by acid treatment facilitates homogeneous dispersion. In contrast, pristine MWCNTs were not dispersed well and settled within few minutes due to the strong van der Waals' forces between the nanotubes.

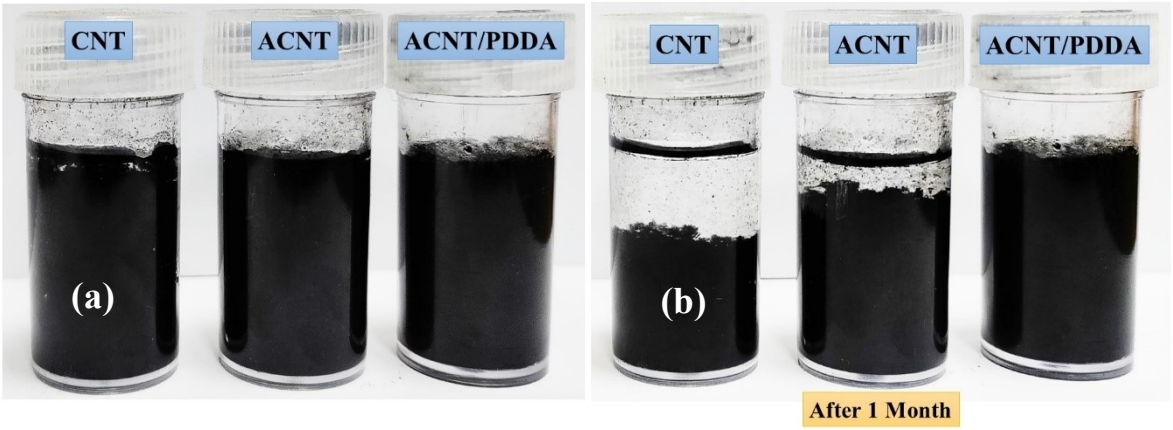

Figure S10. (a) Digital image of the aqueous dispersion of CNT, ACNT and ACNT/PDDA taken immediately after the dispersion and (b) dispersion after 1 month. Since nanoscale defects and functional groups are induced on the surface of pristine MWCNTs by acid treatment, the ACNTs were homogeneously dispersed. However, MWCNTs were not dispersed well and settled due to the strong van der Waals' forces between the nanotubes. The ACNT/PDDA was well dispersed and the suspension was highly stable even after one month.

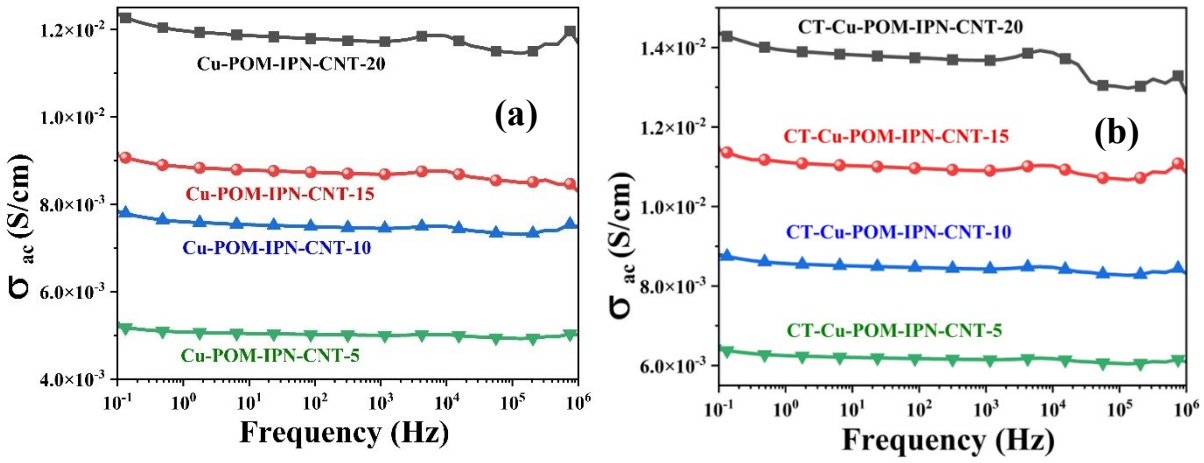

Figure S11. Room-temperature frequency dependent ac conductivity of Cu-POM immobilized IPN-CNT construct having various ACNT/PDDA content (a) before charge triggering and (b) after charge triggering.

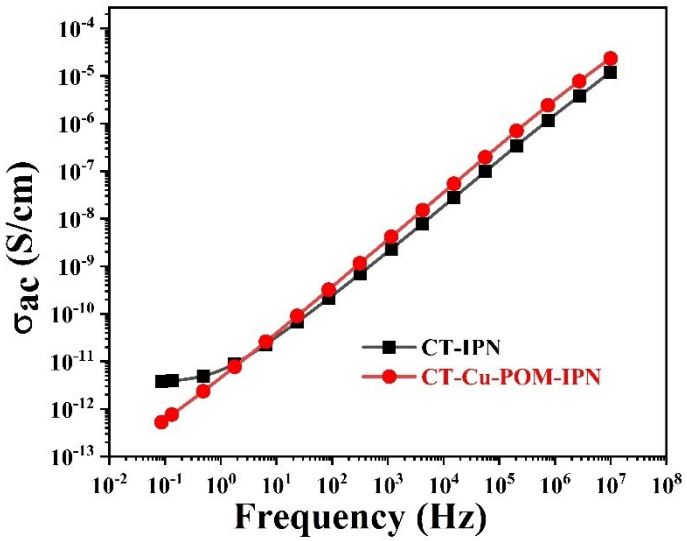

Figure S12. Frequency-dependent room temperature ac conductivity of CT-IPN and CT-Cu-POM-IPN

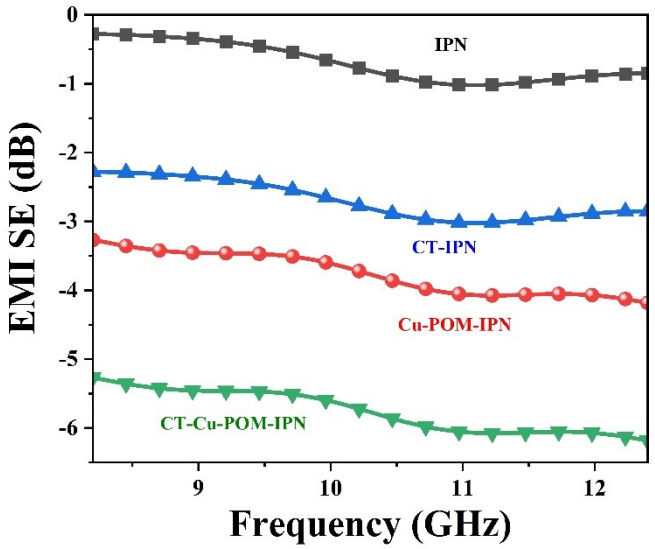

Figure S13. Plot of Frequency vs EMI SE of IPN, CT-IPN, Cu-POM-IPN and CT-Cu-POM-IPN

Supplementary Information IV (SI-4)

Theory of Electromagnetic Interference (EMI) Shielding

EMI SE is the material's ability to attenuate the energy of the incident electromagnetic waves. When the electromagnetic radiations interact with material under test (shield), the shielding phenomenon is governed by the contributions from reflection (SE_R), absorption (SE_A), and multiple internal reflections (SE_M). The total EMI SE (SE_T) is the sum of the contributions from SE_R, SE_A and SE_M. The total SE_T can be written as;

$$SE_T = SE_R + SE_A + SE_M \quad \text{(S1)}$$

For calculations, SE_M is generally considered negligible when SE_T is higher than 15 dB. In a vector network analyzer, EMI SE is represented in terms of scattering parameters which are S_{11} (forward reflection coefficient), S_{12} (forward transmission coefficient), S_{21} (backward transmission coefficient), and S_{22} (reverse reflection coefficient). The SE_T can be evaluated from the S parameters by using the following equations[1]

$$SE_R = 10log\left(\frac{1}{1-R}\right) = 10log\frac{1}{1-|S_{11}|^2} \quad \text{(S2)}$$

$$SE_A = 10log\left(\frac{1-R}{T}\right) = 10log\frac{1-|S_{11}|^2}{|S_{21}|^2} \quad \text{(S3)}$$

Assuming propagation of EM waves in a nonmagnetic and highly conducting medium, the Fresnel formula for reflection, absorption and multiple reflections, using equation S1, can be given as,

$$SE_T = 10log\left(\frac{1}{T}\right) = 10\log\left(\frac{1}{|S_{21}|^2}\right) = 10log\left(\frac{E_i}{E_t}\right)^2 = 20log\left|\frac{(1+N)^2}{4N}e^{-kd}[1-\left(\frac{1-N}{1+N}\right)^2 e^{2ikt}]\right| \quad \text{(S4)}$$

where E_i and E_t are incident and transmitted intensities of electric field of the EM waves, respectively; N is the complex refractive index of the shield, k is the imaginary part of refractive index, and t is the shield thickness.

The EMI Shielding efficiency % can be calculated by the following equation.[2]

$$Shielding\ Efficiency\ \% = 100 - \left(10^{\frac{SE}{10}}\right)^{-1} \times 100 \quad \text{(S5)}$$

Where, SE stands for total shielding efficiency i.e. SE_T

The EMI SE of a material is defined as the material's ability to attenuate the striking EM wave by the aids of R, A and M. Where, R refers to the reflection coefficient or reflectivity, A refers to the absorption coefficient or absorptivity and M multiple internal reflections.

In practice, two-port network model of Vector Network Analyzer (VNA) is used to measure the scattering parameters (S_1, S_{12}, S_{21}, and S_{22}) wherein the reflection R and transmission T coefficients are obtained from these scattering parameters using the following equations.

$$R = |S_{11}|^2 = |S_{22}|^2 \quad \text{(S6)}$$

$$T = |S_{21}|^2 = |S_{12}|^2 \quad \text{(S7)}$$

$$A = 1 - R - T \quad \text{(S8)}$$

Where, S_{11} and S_{21} represent the reflection parameter obtained using VNA port 1 and the transmission parameter from port 1 to port 2, respectively. S_{22} and S_{12} denote the reflection parameter obtained from VNA port 2 and the transmission parameter from

port 2 to port 1, respectively. S_{21} refers to the forward transmission, and S_{12} refers to the reverse transmission. If the shield material is uniform, $S_{11} = S_{22}$ and $S_{21} = S_{12}$. [1,2]
The absorption (SE_A) and (surface) reflections (SE_R), are also estimated from the measured S parameters. If $SE_A \gg 10$ dB, then the SE_M can be neglected and there is an effective absorption A_{eff}, as described by the following equation [1,2]

$$A_{eff}(dB) = \frac{1-(R+T)}{1-R} \quad \text{(S9)}$$

Then, the values of SE_R and SE_A can be calculated by the following equations:

$$SE_R(dB) = 10log\left(\frac{1}{1-R}\right) \quad \text{(S10)}$$

$$SE_A(dB) = 10log\left(\frac{1}{1-A_{eff}}\right) = 10log\left(\frac{1-R}{T}\right) \quad \text{(S11)}$$

and SE_T can be expressed by

$$SE_T(dB) = SE_R + SE_A = 10log\left(\frac{1}{T}\right) \quad \text{(S12)}$$

The green index (g_s) of CT-Cu-POM-IPN-CNT-20 is calculated using Eq. S11 as below:

$$g_s = \frac{1}{S_{11}^2} - \frac{S_{21}^2}{S_{11}^2} - 1 \quad \text{(S11)}$$

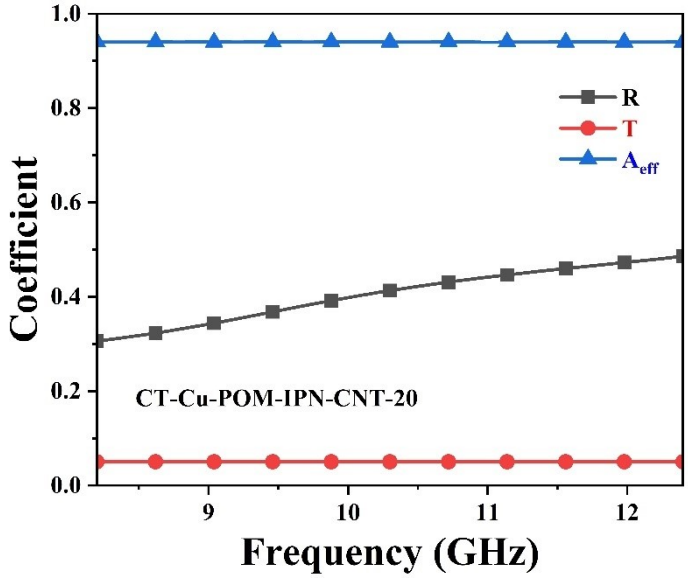

Figure S14: Plot of Reflection (R), Transmission (T) and Effective Absorption coefficient (A_{eff}) of CT-Cu-POM-IPN-CNT-20 vs frequency.

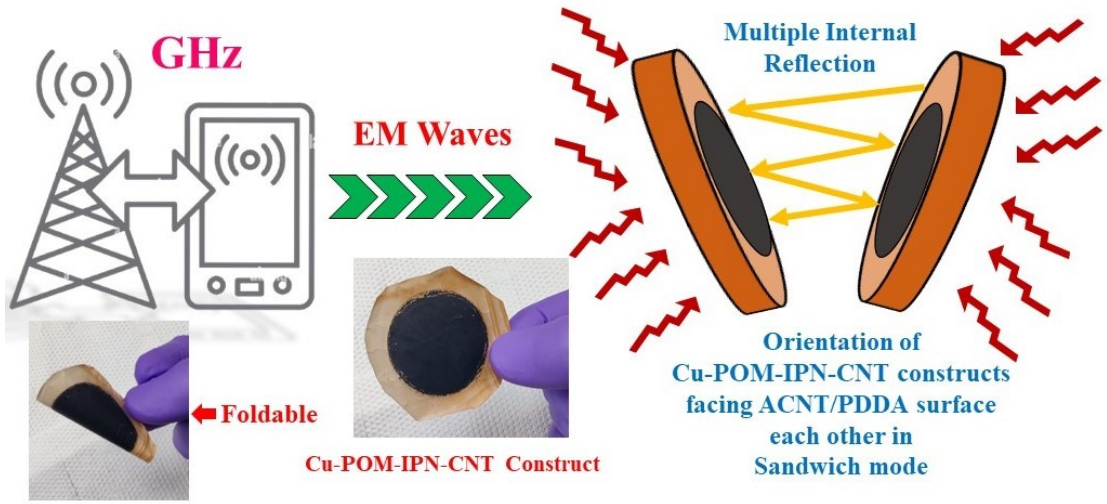

Figure S15. Schematic presentation of multiple internal reflections caused by Cu-POM-IPN-CNT Construct in sandwiched mode.

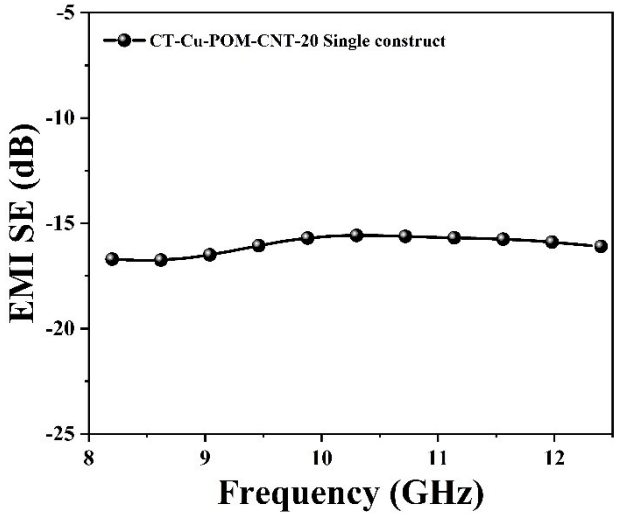

Figure S16. Plot of EMI SE vs Frequency of CT-Cu-POM-CNT-20 single construct.

Supplementary Information V (SI-5)

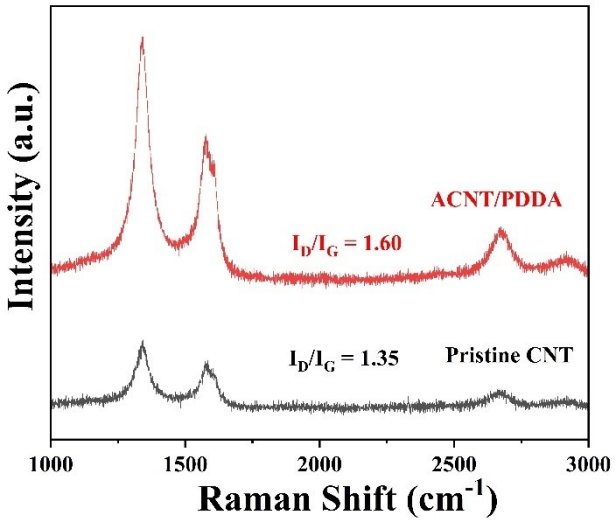

Figure S17. Plot of Intensity vs Raman shift of pristine CNT and ACNT/PDDA

Raman spectroscopic measurements were carried out for the pristine CNT, ACNT, and ACNT/PDDA. As shown in Figure S7, the acid functionalization caused a slight increase in the intensity ratio (I_D/I_G) of the D band ~1340 cm^{-1} to G band ~1577 cm^{-1} for both the CNT and ACNT/PDDA, which was accompanied by the up-shift in G band. The I_D/I_G value which is

proportional to the extent of induced defect corresponds to 1.35 and 1.6 for pristine CNTs and ACNT/PDDA respectively.

References

1. Iqbal, A. *et al.* Anomalous absorption of electromagnetic waves by 2D transition metal carbonitride Ti_3CNT_x(MXene). *Science (80-.).* **369**, 446–450 (2020).
2. Lee, J. *et al.* Ultrahigh electromagnetic interference shielding performance of lightweight, flexible, and highly conductive copper-clad carbon fiber nonwoven fabrics. *J. Mater. Chem. C* **5**, 7853–7861 (2017).